Assessment of Biophysical Soil Properties Through Spectral Decomposition Techniques

A. R. Huete

Department of Soil and Water Science, University of Arizona

R. Escadafal*

ORSTOM, France

A mixture model was utilized to extract soil biophysical properties from fine resolution soil spectra (400–900 nm) measured outdoors with a portable spectroradiometer. The objective of this study was to fully characterize soil spectral signatures in the visible and near-infrared in terms of underlying "basis" curves, key wavelengths, and dimensionality. Through spectral decomposition and mixture modeling, the reflectance response of a wide, genetic range of soil materials were separated into four independent sources of spectral variability (basis curves), which in linear combination were able to reconstitute the experimental data set. Stepwise spectral reconstruction was then utilized to isolate organic carbon and free iron oxide "basis" curves. This enabled a good "global" measure of soil properties irrespective of soil type or brightness. We anticipate the EOS-MODIS and HIRIS sensors to provide the spectral data needed for inversion of satellite data into soil surface properties and processes.

INTRODUCTION

Soils are a heterogenous, polyphasic combination of solid mineral and organic constituents, liquid, and gas. A typical soil may consist of 50% pore space with spatially and temporally variant proportions of gas and liquid. The solid phase consists of a complicated genetic mixture of primary minerals in the sand and silt fractions, clay minerals, organic polymers, and secondary mineral coatings. With the inclusion of rocks, litter, and various roughness conditions at the surface, one finds a complex reflectance response from soil surfaces with additional spatial and temporal variance patterns at all scales.

The aim of remote sensing methodologies is to exploit these patterns of energy interactions for the purpose of extracting the most information about the biophysical character of soil surfaces. The aim of the soil scientist, in turn, is to extend these spatially measured, noninvasive techniques

*Currently visiting scientist at the University of Arizona

Address correspondence Dr. A. R. Huete, Dept. of Soil & Water Science, 429 Shantz Bldg., #38, University of Arizona, Tucson, AZ 85721.

149

below the surface so as to describe the soil as a dynamic, three-dimensional natural body with spatially variable properties.

The noninvasive measurement of soil properties is normally accomplished with measurements of solar reflected and emitted electromagnetic radiation from the soil surface. The spectral composition and intensity of this energy are related to the biological and mineralogical properties of the soil surface and are interdependent with external solar/view angles and atmosphere.

Soil Spectral Variance

Both the intensity (brightness) and spectral composition of reflected energy are useful in describing the optical behavior of a soil. Brightness represents the dominant or principal source of spectral variance among soils whereas spectral curve shape differences are secondary. Spectral variations are normally associated with specific absorption phenomena and are often quantified through the use of waveband ratios. The general shape of a spectral curve provides information on the size, geometry, and surface composition of the particles. In the visible portion of the spectrum, absorption features among soils are not generally sharp but instead are weak and broad.

There are many laboratory experiments on soil reflectance patterns (Bowers and Hanks, 1965). Obukhov and Orlov (1964) presented three soil curve types in the spectral range from 400 nm to 800 nm. These included monotonically rising curves, low reflecting, slightly concave curves, and sigmoidal curve forms which show absorption in the shorter wavelength range and high reflection in the yellow and red wavelengths. Condit (1972) visually classified 160 soil response curves into a similar set of three basic curve types. Stoner and Baumgardner (1981) presented five soil spectral shapes from a study involving 485 wetted soils over a larger portion of the spectrum (0.52–2.32 μm).

In these studies, no attempts were made to quantitatively relate spectral shape to soil properties. Furthermore, there were often problems in assigning soils to such discrete curve types. Courault et al. (1988) used the curve shape of soil spectra as a first approximation in assessing soil composition and physical characteristics. They analyzed 84 soil samples with a spectrophotometer

and identified six classes of curves in the visible (400–700 nm). As in the previous studies, organic carbon, iron oxides, and carbonates were the main soil constituents responsible for curve shape classification schemes. Soils rich in organic carbon frequently have concave reflectance curves between 0.5 μm and 1.3 μm whereas soils low in organic carbon show convex and/or sigmoidal curves. If iron and organic carbon are the main constituents responsible for soil spectral curve shapes, then it may be possible to discriminate soils in accordance with their curve form and assess their chemical makeup.

The analysis of the curve shape in the visible portion of the spectrum also enables the extraction of soil color information which is often related to soil properties (Escadafal et al., 1988; 1989). Munsell hue and chroma differences manifest themselves as curve shape variance in the visible whereas brightness variations would be associated with Munsell color "value" (Munsell Color Co., 1950).

Spectral Mixture Modeling of Soil Surfaces

Spectral decomposition methods and mixture modeling of soil surfaces provide an exploratory method to a) uncover complex interrelationships among spectral phenomena, b) discern independent patterns of soil spectral behavior, and c) mold findings into predictive models. The technique involves the decoupling of soil spectra into a set of simplified parameters, related to specific soil spectral features, that lend themselves to physical models. The ability to describe complex response functions by a small number of parameters facilitates the search for relationships among the observed response variations and the causal variables of the experiment (Huete, 1986). In this way, one may find underlying factors and isolate subtle curve influences responsible for soil spectral differences and one may fully examine the potential for remotely sensed data to characterize soil surface properties and condition.

Two types of spectral mixture models, macroscopic and intimate (Smith et al., 1985), are applicable to the study of soil spectra. In a macroscopic mixture, homogeneous patches of different soil types or moisture contents are present within a pixel and independently contribute toward the measured response. An intimate mixture, by con-

trast, involves first and second order multiple scatterings of radiant energy among the pixel components such as in soil particle coatings of secondary minerals and humic substances. Intimate mixtures are nonlinear combinations of component spectra whereas macroscopic mixtures involve additive, linear combinations of the subpixel constituents (Smith et al., 1985). The components of a mixture model are generally labeled as endmembers and may be "pure" or an aggregate of several components.

Since iron oxides and humic substances tend to be ubiquitous in soil substrates, soils are rarely pure and it becomes difficult to define appropriate endmember or reference spectra from which one could describe either the response of an individual soil or the spectral characteristics of a global range of soil types. Thus far, soil spectra behavior has been analyzed in terms of specific biophysical properties or in terms of spectral classification schemes, which in turn are correlated with climatic and genetic environmental factors.

THEORY

The basis of the mixture model presented here is that soil responses are treated as mixtures of various soil spectral properties. Soil spectral response is equal to the weighted sum of unique reflecting soil features:

$$d_{i,k} = \sum_{j=1}^{n} r_{i,j} c_{j,k}, \qquad (1)$$

where $d_{i,k}$ is the measured response of soil k in waveband i, n is the number of unique spectral features in the soil population, $r_{i,j}$ is the response of feature j in waveband i, and $c_{j,k}$ is the loading or contribution of feature j in soil k. In matrix notation, Eq. (1) is expressed as

$$[D] = [R][C], \qquad (2)$$

where D is the experimental data matrix, R is the response or eigenspectra matrix of independent "basis" spectral curves, and C is the eigenvector matrix consisting of the contributions or scalar multiples of each "basis" curve to the experimental data.

Principal components analysis is initially used to decompose the data matrix D into an abstract eigenspectra matrix R_A and abstract eigenvector matrix C_A such that $[D] = [R]_A[C]_A$. Mathematically, this is accomplished by solving the eigenvalue problem:

$$[Z]_0[C]_A = [\lambda][C]_A, \qquad (3)$$

where Z is a symmetric covariance about the origin matrix with no data preprocessing ($Z_0 = D^T D$) and λ is a diagonal matrix of eigenvalues. The abstract eigenspectra matrix is then constructed according to

$$[R]_A = [D][C]_A^T, \qquad (4)$$

where $C^{-1} = C^T$ for orthonormal matrices.

The eigenvalues, which are extracted in order of importance, are used to extract an intrinsic minimum number of basis curves which account for all curve shape differences in the experimental data (Simonds, 1963). Knowing the dimensionality of a soils data set also aids in determining the number of wavebands, their locations, and resolutions needed to fully characterize a soil and derive maximum soils information.

One method to find n is to reconstruct the data matrix, according to Eq. (1), following each eigenvalue extracted (Weiner et al., 1970). The stepwise, data reconstruction procedure begins with $n = 1$, that is, only the eigenvector and eigenspectra, corresponding to the largest eigenvalue, are used:

$$d_{i,k} = r_{i,1} c_{1,k}. \qquad (5)$$

If the calculated data set agrees with the experimental data set to within experimental error, the number of unique reflecting components, n, is 1. If not, then the next most important eigenvector and eigenspectra are included in the computation:

$$d_{i,k} = r_{i,1} c_{1,k} + r_{i,2} c_{2,k}. \qquad (6)$$

This is continued until the regenerated data set is in agreement with the experimental data set. At each step of the data reproduction procedure, the residual standard deviation (RSD) is calculated to provide a measure of the deviation of the regenerated data matrix from the experimental data matrix (Malinowski and Howery, 1980);

$$RSD = \left[\frac{\sum_{j=n+1}^{c} \lambda_j}{r(c-n)} \right]^{1/2}, \qquad (7)$$

where r and c represent the size of the data matrix with $r > c$.

The "basis" response curves (eigenspectra) provide efficient representation of the experimen-

tal data, but there is no certainty that there will be a simple relationship between these curves and underlying causal, biophysical variables. Condit (1972) applied eigenvector analysis to the study of soil spectra and found that the 160 sets of dry soil spectra curves could be reduced to four "basis" response curves plus a mean soil curve, which, in linear combination, could reproduce the entire family of soil response curves. More recently, Price (1990) studied the spectral variability (0.55–2.32 μm) of over 500 soils and found that four "basis" vectors were sufficient to describe the entire set of soil spectra. However, neither Price (1990) nor Condit (1972) made an attempt to physically relate these basis curves to specific soil properties.

In this paper, a family of soil response curves are decomposed into fundamental and unique, basis curves. A mixture model is then utilized for the extraction of soil biophysical properties based upon the amounts of each basis curve needed for reconstitution of experimental soil spectra. In addition, the location and number of wavebands necessary for soil spectral characterization are investigated and the development of appropriate "endmembers" for global scale mixture modeling are considered.

METHODOLOGY

Forty-six soils in air-dry, sieved condition (< 2 mm to remove gravels and rocks) were measured in 10 nm wavelength intervals from 400 nm to 900 nm with a field portable spectroradiometer. Nadir view reflectance responses were measured from a height of 42 cm, outdoors on cloudless days at a nominal solar zenith angle of 40°. Reflectance factors were obtained by ratioing the reflected response from a soil by that of a reference panel with reflectance adjusted for sun angle.

The soils were collected from various biome types (temperate desert, semidesert grassland, oak woodland, pine forest, and tropical grassland) in the midwest, Sonoran desert, Basin and Range Plateau, and Hawaii, U.S.A. The soils varied from undeveloped (shallow) Entisols and Inceptisols to fully weathered (deep) Oxisols. Included in the set of experimental measurements were 10 soils from a climosequence along the Santa Catalina Mountains near Tucson, Arizona (Galioto, 1985). All soils along this sequence were formed from similar

Table 1. Soils and Vegetation from a climosequence in the Santa Catalina Mountains (Whittaker et al., 1968)

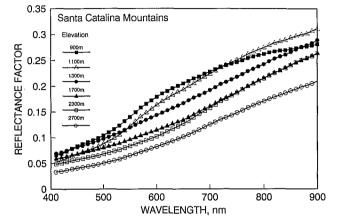| Elevation (m)	Vegetation	Classification (U.S. Soil Taxonomy)	% O.C.
900	desert scrub	Lithic Haplargid	0.46
1100	desert grassland	Lithic Torriorthent	0.55
1300	open oak woodland	Lithic Ustorthent	1.33
1700	pine-oak woodland	Lithic Ustorthent	3.91
2300	pine forests	Typic Ustochrept	5.85
2700	subalpine forest	Typic Haploboroll	7.90

Figure 1. Spectral reflectance signatures for soils along the Santa Catalina climosequence.

genetic material but vary in organic carbon content in response to annual precipitation (27–85 cm at high elevations) and temperature differences (Table 1). A sample of the variation in spectral signatures along this transect is shown in Figure 1.

To further illustrate the spectral variance in the soils population, the five most unique spectral curves and their characteristics are shown in Figure 2 and Table 2. In the mixture decomposition process these are named "key" soils because they account for nearly all of the variance encountered in this study and all other soil signatures may be approximated by some linear combination of these five soils.

The three spectral curve forms described by Obukhov and Orlov (1964) and Condit (1972) are readily apparent; the convex curve form (Karro), resembling a minimally altered, calcareous soil, the concave curve form [Santa Catalina (S.C.) 2300 m] representative of organic rich soils, and the sigmoidal curve forms which are affected by free iron oxide coatings on soil particle surfaces. The position of the inflection point and plateau, however, vary over the three sigmoidal curve forms.
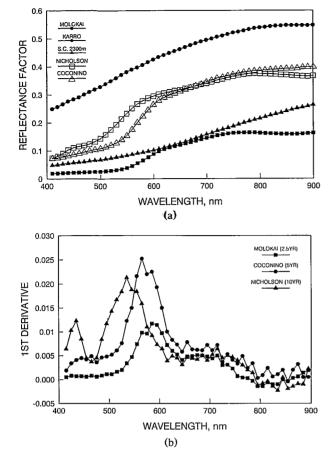
Figure 2. (a) Spectral reflectance signatures of the five "key" soils and (b) the first derivative spectra for the three iron-affected, sigmoidal curve forms.

Table 2. Characteristics of the Five Key Soils in This Study

Soil Series	Soil Classification	Soil Color
Nicholson	Typic Fragiudalf (yellowish brown)	10 YR 5/4 (fine-silty, mixed, mesic)
Molokai	Typic Torrox (clayey, kaolinite, isohyperthermic)	2.5 YR 3/4 (dark reddish brown)
Karro	Ustollic Calciorthid (fine-loamy, carbonatic, thermic)	10 YR 7/2 (light gray)
Coconino	red fine sand (not classified)	5 YR 5/5 (yellowish-red)
Santa Catalina	Typic Ustochrept (loamy skeletal)	7.5 YR 3/2 (dark brown)

The first derivative spectra highlights these different inflection points (Fig. 2b) with the peaks shifting toward longer wavelengths with respective soil hues (Table 2) of yellow (Nicholson, 10YR), yellow-red (Coconino, 5YR), and red (Molokai, 2.5YR).

Table 3. Decomposition of Soil Reflectance Data Set

No.	Eigenvalue	Real Error	Key Band (nm)	Condit (1972) (nm)
1	119.6260	0.0187	410	400
2	0.5753	0.0098	900	920
3	0.1788	0.0038	610	640
4	0.0252	0.0017	540	540
5	0.0045	0.0008	780	740
6	0.0008	0.0005	480	
7	0.0002	0.0004	450	
8	0.0001	0.0004	570	

RESULTS

Mixture Decomposition

The results of the decomposition procedure (46 soils × 50 bands) are summarized in Table 3. The eigenvalues are the orthogonal variances of the data matrix ranked in order of magnitude. The dimensionality of the data set is not easy to determine; however, by using the real error criteria, the dimensionality may be estimated to be 4 or 5 depending on the acceptable level of experimental error. With four "basis" curves, the population of soil spectra signatures may be regenerated to within ±0.17% reflectance and, with the inclusion of the fifth basis curve, the soil spectral signatures could be regenerated to within ±0.08% reflectance.

The entire soil experimental data set could thus be represented as mixtures of four or five basis curves (eigenspectra). Similarly, we may also state that four or five "key" bands are needed to completely characterize and reconstruct a soils spectrum. The "key" bands, in order of importance, are shown in Table 3 along with those reported by Condit (1972). Both sets appear similar and, since soil spectral features tend to be coarse, there is some flexibility in the exact positioning and spectral resolution over these five bands.

Eigenspectra (Basis) Curves

Figure 3 shows the resulting five, unique "basis" curves (eigenspectra). In contrast to the five "key" soil signatures (Fig. 2a), these curves are totally uncorrelated with one another. Furthermore, all measured soil curves can be reconstituted from linear combinations of these curves. Ideally, each eigenspectrum represents a unique soil spectral
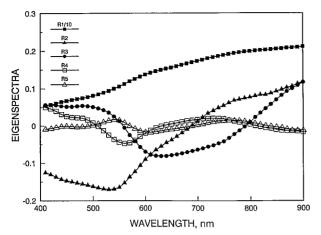
Figure 3. The first five eigenspectra (basis) curves following decomposition of the soil experimental data set.

spectra curves regenerates the soils population to within ±0.38% reflectance.

Eigenspectrum 4 is similar to the absorptance spectrum of goethite, a yellow, "reduced" form of iron oxide with absorption regions at approximately 460 nm and 560 nm (Hunt et al., 1971; Kosmas, 1984). The spectral feature in the 520–600 nm region has the effect of adding or subtracting "green" to a soil's signature enabling discrimina-
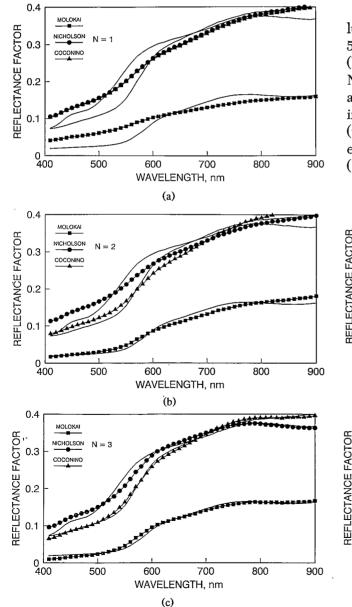
Figure 4. Stepwise regeneration of the soils along the Santa Catalina climosequence for (a) $n = 1$, (b) $n = 2$, and (c) $n = 3$. (Lines with symbols represent regenerated spectra; lines without symbols are experimental spectra.)

property and the amount of each curve needed to reconstitute a soil signature is a measure of the significance of that property in the soil sample.

The first eigenspectrum curve (R1) is slightly sigmoidal and represents the best fit or "mean" soil curve for the soils population. This curve characterizes the most dominant soil spectral property, namely its brightness. The amount of this curve needed to approximate a particular soil signature is a measure of that brightness and is quantified in the loadings matrix (C1). The entire soil spectral population can be reconstituted to within ±1.87% reflectance (Table 3) by multiplying the first eigenspectrum and first eigenvector [Eq. (5)].

The second eigenspectrum (R2, Fig. 3) has a strong absorption region at 540 nm and a slight (broad) absorption at around 820 nm, both of which resemble the spectral behavior of iron oxides (Hunt et al., 1971; Kosmas et al., 1984). The addition of this "iron oxide" curve with the first, mean soil curve regenerates all soil spectral signatures to within ±0.98% reflectance [Eq. (6)]. In a color sense soils become redder with the addition of this curve to the "mean" soil signature (R1) since green and blue responses are being subtracted relative to the red and near-infrared.

The third eigenspectrum curve (R3, Fig. 3) has a concave shape resembling the organic dominated soil curves of Stoner and Baumgardner (1981) and Condit (1972). This signature may thus be needed to model the influence of decomposed organic constituents on soil spectral behavior and the inclusion of the curve with the first two eigen-

(a)

(b)

(c)

tion between the red and yellow forms of free iron oxides in soils. With the above four "basis" curves in a mixture model, the soil population of spectral signatures can be reconstituted to within $\pm 0.17\%$ reflectance.

Eigenspectrum 5 has peaks at 550, minima at 600 nm, and a broad peak at 770 nm. It is not clear what the fifth eigenspectrum curve represents or if it is necessary for soil spectra regeneration. In the next section, soil signatures are regenerated and compared with the experimental data to further assess the dimensionality of the data set.
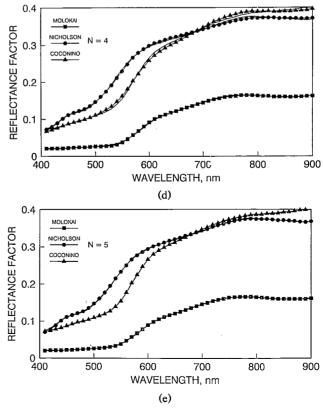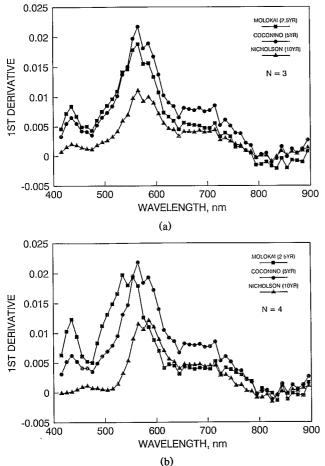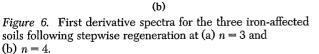
Data Regeneration

Figure 4 shows the stepwise regeneration of the Santa Catalina climosequence using one, two, and three component mixture models. The spectral signature of the desert soil (S.C. 900 m) is reconstituted fairly well with only the first eigenspectrum (Fig. 4a) but the organic enriched soils, at 2300 m and 2700 m elevation, are poorly reproduced. Inclusion of the second eigenspectrum (red iron oxide "basis" curve) did little to improve soil spectral regeneration (Fig. 4b); however, by adding the third eigenspectrum organic "basis" curve, the organic enriched soils of the climosequence were reproduced nearly entirely (Fig. 4c). This gives support to the third eigenspectrum representing an isolated organic "basis" curve.

The same data reconstruction procedure is illustrated for the iron-affected "key" soils in Figure 5. All three soils are poorly described by the first (brightness) eigenspectrum (Fig. 5a) and the Nicholson and Coconino soils are indistinguishable. Inclusion of the second eigenspectrum (red iron oxide curve) had little effect on the Nicholson (yellow soil) but significantly improved the regeneration of the reddish Coconino and Molokai soils (Fig. 5b). The Nicholson and Coconino are now

Figure 5. Stepwise regeneration of three iron-affected, key soils; (a) $n = 1$; (b) $n = 2$; (c) $n = 3$; (d) $n = 4$; (e) $n = 5$. (Lines and symbols as in Fig. 4.)

Figure 6. First derivative spectra for the three iron-affected soils following stepwise regeneration at (a) $n = 3$ and (b) $n = 4$.

Figure 7. Relationship between % soil organic carbon and (a) C1 loadings and (b) C3 loadings.

discriminable and the iron-rich Molokai is regenerated fairly well.

The addition of the third eigenspectrum (organic basis curve) further improves the modeled spectra (Fig. 5c); however, the fourth eigenspectrum (yellow iron oxide basis curve) provides for nearly complete data reconstitution, especially in the case of the yellow-colored Nicholson soil (Fig. 5d). The importance of the fourth basis curve in modeling iron-affected soils is demonstrated by plotting the first derivative spectra for the regenerated spectra at $n = 3$ and $n = 4$ (Fig. 6). With a three-component model the primary curve peaks are not discriminable, but upon inclusion of the fourth curve, the three iron-affected, yellowish to red colored soils separate out.

Figure 5e shows a small degree of data modeling improvement resulting from the inclusion of the fifth eigenspectrum curve. In analyzing Figures 4 and 5, it would appear that a four-compo-
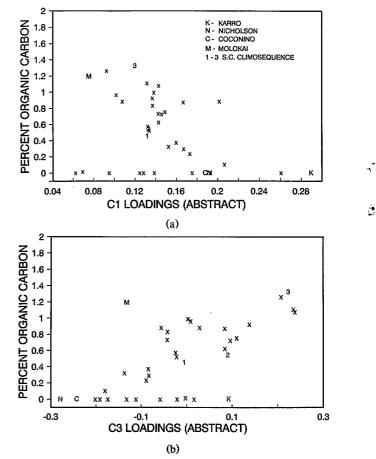
nent mixture model is sufficient to adequately describe the soil spectral information content (46 soils) encountered in this study, that is, the model improvement resulting from the fifth basis curve is small relative to anticipated or encountered experimental error.

Soil Biophysical Properties

To a certain extent, the spectral decomposition process has isolated various soil spectral features relevant to the assessment of soil properties. The loadings (C3) of the organic basis curve (R3) needed for regeneration of a soil spectral signature is related to the soil's organic carbon content. The R3 eigenspectrum has a concave curve shape and is independent of the usual measure of soil organic carbon, the brightness curve (R1). Thus, we now have two independent measures of a soil's organic carbon status (Figs. 7a and 7b) with the C3 loadings producing a slightly improved correlation ($r = 0.71$) over the C1 loadings ($r = 0.57$). The C3

loadings also respond to slight changes in organic carbon over the Santa Catalina (S.C.) 1, 2, and 3 sequence (900, 1100, and 1300 m elevation), where the C1 loadings appear insensitive.

In contrast to the C1-brightness loadings, however, the C3 loadings would not be affected by soil moisture, roughness, shading, or other brightness-related influences. This is because brightness (R1) is a measure of the amplitude of a soil spectral signature while the third eigenspectrum (R3) is a measure of the concavity of the signature. Since the numerous factors which alter the brightness of soils do not affect the soils' concavity, the C3 loadings would be a more reliable measure of soil organic carbon. As with the brightness measure, the C3–organic carbon relationships breaks down beyond 2% organic carbon where most soil particle surfaces become fully coated with humic material. The corresponding organic carbon correlations for all soils are: for C1, $r = 0.42$ and for C3, $r = 0.64$. The textural attributes of a soil also modify such relationships and contribute to the scatter in the plots.

Figure 8a is a C3–C4 plot showing the loadings or amounts of the third (organic carbon) and fourth (iron) "basis" curves present in all 46 soil signatures. As the C3 loadings increase, particularly over the Santa Catalina climosequence from low to high elevations (1–6), organic humus coatings mask the iron and other mineral spectral features and C4 loadings converge toward zero. With convergence, soil chromas (Fig. 8b) drop to low values (gray colors) due to the darkening effect of humus. At low C3 loadings, the influence of organic carbon is reduced and iron-related spectral features and colors stand out. The C4 axis separates red and yellow hues (Fig. 8c) in accordance with the type of iron oxide (oxidized or reduced) and soil chromas become higher with lower C3 loadings.

In conclusion, high resolution spectra in the region from 400 nm to 900 nm does provide important information about a soil's organic carbon and iron contents. An organic "basis" curve as well as red and yellow curve forms of iron oxides are extractable across a broad range (global) of soil types formed under a variety of genetic materials. This provides a means for analyzing soil properties based on high resolution spectral curve shapes, irrespective of the "brightness" or intensity of the signature.
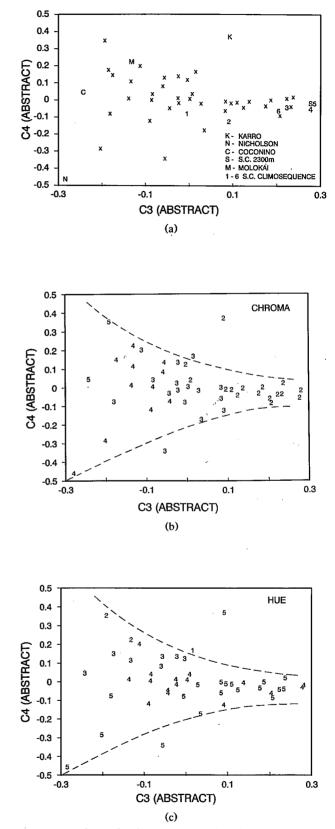

Figure 8. Relationship between C3 and C4 loadings for (a) the soils population and for (b) Munsell chroma and (c) Munsell hue with $1 = 10R$, $2 = 2.5$ YR, $3 = 5$ YR, $4 = 7.5$ YR, $5 = 10$ YR.

DISCUSSION

In this study, spectral decomposition and mixture modeling were utilized to determine independent, global patterns of soil spectral behavior and isolate subtle curve shape influences. Four characteristic basis curves, independent of each other, were determined essential for spectral reconstruction of the entire family of soil spectral signatures. Spectral isolation of these unique "basis" curves not only aided in the assessment of the dimensionality of soil spectra, but also provided for an analysis of the "physical" importance of each basis curve toward soil spectral behavior. This enabled weak and broad absorption features in soil spectral signatures to be isolated from the dominant brightness component as each basis curve became vital in understanding and modeling soil spectral behavior.

For example, without the organic basis curve, one cannot reconstitute most soil spectral signatures, particularly those with appreciable amounts of organic carbon ($\sim 0.5\%$). Since the majority of soils on this planet possess some amount of organic carbon, this third basis curve is vital toward spectral characterization of the global soils population. Thus, soil organic carbon could be assessed and differentiated from soil color and brightness variations caused by moisture, roughness, and illumination conditions.

Similarly, the red and yellow forms of free iron oxide "basis" curves were essential in describing the "global" population of soil spectra. If one were in an arid region with well-aerated soils (red iron oxides), the fourth basis curve or even the third organic basis curve may not be necessary to describe regional soil conditions. However, in global studies one needs to extrapolate results across biome types and all unique soil spectral features must be accounted for. The basis curves derived from this experimental data matrix may also be used to create new spectral signatures from soils not included in the original soil data set. If new data cannot be fitted by the established basis curves, then the new data is from a different population of response variability.

As seen in this study, there are two possible classes of endmembers which may be utilized in soil mixture models, namely, a) discrete soil types (key soils) with unique curve forms and b) pure signatures of unique soil spectral properties. Fig-ure 2 is an example of key soils which could serve as endmembers in a mixture model scheme. In a global sense and as concluded by Stoner and Baumgardner (1981), only a discrete number of soil curve forms exist and hence are truly separable. However, each unique soil curve form represents some mixture of soil properties (iron, organics, etc.). It may also be unrealistic to model soil spectral response curves in this manner since there may exist a continuum of response curves between any two unique soil curve types, such as in the climosequence (Fig. 1). In transition zones involving more than one soil type, various soil associations may be encountered within a pixel producing a range of composite soil signatures. Two soil types within a pixel may not be separable unless they possessed unique spectral curve forms.

On the other hand, it may be easier to isolate soil spectral properties such as organic carbon and iron oxides across the various soil curve types. In this case, the eigenspectra or "basis" response curves (Fig. 3), which are independent of soil curve type or key soils, are used as endmembers to model soil biophysical properties. The loadings thus represent a measure of soil properties relative to the abstract eigenspectra signature. The transformation of the abstract to a "real" solution with physical significance can be accomplished through rotation of the eigenspectra to line up, in a least squares sense, with the spectral signatures of reference of pure materials that are already physically and chemically characterized. Ideally, pure humus, hematite (red iron oxide), and goethite (yellow iron oxide) spectral signatures would provide the means for deriving the "real" mixtures solution. The loadings would then measure the corresponding soil properties relative to the reference signature rather than the abstract eigenspectra signature.

It is hoped that high resolution sensors such as HIRIS (Goetz and Herring, 1989) would allow for a complete global soils characterization with a thorough dimensionality analysis, extraction of key "basis" curves, and definition of endmembers. Once the number and necessary wavelength regions are known for soil differentiation and spectral property extraction, it is hoped that coarser resolution spectra, such as may be obtained by MODIS-N and -T (Salomonson et al., 1989), would be sufficient for continual assessment of soils and vegetation within biome types.

REFERENCES

Baumgardner, M. F., Kristoff, S. J., Johannsen, C. J., and Zachary, A. L. (1970), Effects of organic matter on the multispectral properties of soils, *Proc. Indiana Acad. Sci.* 79:413–422.

Bowers, S. A., and Hanks, R. J. (1965), Reflection of radiant energy from soils, *Soil Sci.* 100:130–138.

Condit, H. R. (1972), Application of characteristic vector analysis to the spectral energy distribution of daylight and the spectral reflectance of American soils, *Appl. Opt.* 11:74–86.

Courault, D., Girard, M., and Escadafal, R. (1988), Modélisation de la couleur des sols par télédétection, in *Proc. 4th Int. Colloq. on Spectral Signatures of Objects in Remote Sensing*, Aussois, France, ESA SP-287.

Escadafal, R., Girard, M., and Courault, D. (1988). La couleur des sols: appréciation, mesure et relations avec les propriétés spectrales, *Agronomie* 8:147–154.

Escadafal, R., Girard, M., and Courault, D. (1989), Munsell soil color and soil reflectance in the visible spectral bands of Landsat MSS and TM data, *Remote Sens. Environ.* 27:37–46.

Galioto, T. R. (1985), The influence of elevation on the humic-fulvic acid ratio in soils of the Santa Catalina Mountains, Pima County, Arizona, Ph.D. dissertation, University of Arizona, 112 pp.

Goetz, A. F. H., and Herring, M. (1989), The high resolution imaging spectrometer (HIRIS) for EOS, *IEEE Trans. Geosci. Remote Sens.* 27:136–144.

Huete, A. R. (1986), Separation of soil-plant spectral mixtures by factor analysis, *Remote Sens. Environ.* 19:237–251.

Hunt, G. R., Salisbury, J. W., and Lenhoff, C. J. (1971), Visible and near-infrared spectra of minerals and rocks: III, oxides and hydroxides, *Mod. Geol.* 2:195–205.

Kosmas, C. S., Curi, N., Bryant, R. B., and Franzmeier, D. P. (1984), Characterization of iron oxide minerals by second-derivative visible spectroscopy, *Soil Sci. Soc. Am. J.* 48:401–405.

Malinowski, E. R., and Howery, D. G. (1980), *Factor Analysis in Chemistry*, Wiley, New York, 251 pp.

Munsell Color Co. (1950), *Munsell Soil Color Charts*, Munsell color, Macbeth Division of Kollmorgen Corporation, Baltimore, MD, revised 1975.

Obukhov, A. I., and Orlov, D. S. (1964), Spectral reflectivity of the major soil groups and possibility of using diffuse reflection in soil investigations, *Sov. Soil Sci.* 2:174–184.

Price, J. C. (1990), On the information content of soil reflectance spectra, *Remote Sens. Environ.* 29: (forthcoming).

Salomonson, V. V., Barnes, W. L., Maymon, P. W., Montgomery, H. E., and Ostrow, H. (1989), MODIS: advanced facility instrument for studies of the earth as a system, *IEEE Trans. Geosci. Remote Sens.* 27:145–153.

Simonds, J. L. (1963), Application of characteristic vector analysis to photographic and optical response data, *J. Opt. Soc. Am.* 53:968–974.

Smith, M. O., Johnson, P. E., and Adams, J. B. (1985), Quantitative determination of mineral types and abundances from reflectance spectra using principal components analysis, in *Proc. Lunar Planet. Sci. Conf. 15th, Part 2, J. Geophys. Res.*, 80 (*Suppl.*): C797–C804.

Stoner, E. R., and Baumgardner, M. F. (1981), Characteristic variations in reflectance of surface soils, *Soil Sci. Soc. Am. J.* 45:1161–1165.

Weiner, P. H., Malinowski, E. R., and Levinstone, A. R. (1970), Factor analysis of solvent shifts in proton magnetic resonance, *J. Phys. Chem.* 74:4537–4542.

Whittaker, R. H., Buol. S. W., Niering, W. A., and Havens, Y. H. (1968), A soil and vegetation pattern in the Santa Catalina Mountains, Arizona, *Soil Sci.* 105:440–450.